

Effect of Reaction Temperature on Structural and Optical Properties of CuS Nanoparticles

Yukti* & Neena Jaggi

Department of Physics, National Institute of Technology Kurukshetra, 136 119, India

Received: 10 May 2023; Accepted: 30 May 2023

The present study exploits the hydrothermal method to synthesize Covellite CuS nanoparticles. To optimize the synthesized nanoparticles for their application in Blue Light Emitting Diode (BLEDs), the effect of reaction temperature on their structural and optical properties was studied at 100°C, 125 °C, and 150 °C for 12h. The diffraction and morphological studies were conducted using X-Ray Diffraction and Scanning Electron Microscopy analysis, respectively. The particle size increases with the increase in reaction temperature, and the structural parameters match well with the covellite CuS hexagonal phase prepared at 125 °C. Ultraviolet-visible absorption studies reveal that the bandgap of nanoparticles was found in the range of 2.9-3.1 eV. The Photoluminescence spectroscopy and CIE chromaticity plot show that the sample synthesized at 125 °C has a low recombination rate and emits light in the blue region, suggesting that it can be utilized in devices like BLEDs and lamps.

Keywords: Hydrothermal, Metal Chalcogenides, Covellite Copper Sulphide, Photoluminescence, LEDs

1 Introduction

In recent years, metal chalcogenides-based nano-material have attracted attention owing to their properties like surface-to-volume ratio and quantum confinement which are different from their bulk counterparts. Among different metal chalcogenides, metal oxide and metal sulphides are of great interest as they show fascinating electrical, magnetic, chemical, optical, and morphological properties¹⁻⁶. CuS has attracted the substantial concern of researchers over the past few decades as it is a non-toxic p-type semiconductor. It shows a band gap ranging from 1.2- 2.3 eV, which can be tuned with various stoichiometric compositions djurleite (Cu_{1.9}S), anilite (Cu_{1.75}S), spionkopite (Cu_{1.4}S), yarrowite (Cu_{1.12}S), chalcocite (Cu₂S), digenite (Cu_{1.8}S), geerite (Cu_{1.6}S), covellite (CuS)⁷⁻⁹. It exists in various morphologies such as nanosphere, nanoflower, nanorods, hollow spheres, nanoflakes, nanoplates, etc¹⁰⁻¹³. There are variety of preparatory routes for synthesis of CuS nanoparticles which include microwave, co-precipitation, sol gel, solvothermal/hydrothermal, sonochemical, solid state, ultra-sonic, and many more¹⁴⁻¹⁹. It has potential applications in fields like photocatalysis, gas sensors, solar radiation absorber, optical sensor, LEDs, and many more^{4, 20-23}. Mohamed Bakr Mohamed et al. synthesized ZnS/PVA nanocomposite via thermolysis technique and studied

the effect of calcination at various temperatures from 300 °C to 600 °C, at 600 °C ZnS got converted to ZnO. He observed the enhancement of PL intensity with increased calcination temperature due to the reduction of defect concentration²⁴. Abimbola E. Oluwalana et al. considered the effect of temperature and capping agents on SnS nanocrystals. They studied the decrease in bandgap and intensity of PL emission with rise in temperature²⁵. R. Seoudi et al. examined that during the preparation of nanoparticles, the temperature change influenced the particle size of CdS and ZnS²⁶. Monalisha Goswami et al. examined a decrease in bandgap energy of ZnO nanoparticles. The nanoparticles are slightly shifted in the absorption peak with increasing annealing temperatures. This is ascribed to an increase in crystallite size and defects, which leads to an increase in PL intensity at different annealing temperatures²⁷.

Mohana Priya Subramaniam et al. synthesized SnO nanoparticles using sol-gel method and investigated the effect of pH and annealing temperature on their properties²⁸. S. Abbas et al. characterized CdO nanoparticles prepared by co-precipitation method under different pH and varying the calcination temperatures²⁹.

In the present work, authors have synthesised the covellite copper sulphide nanoparticles via hydrothermal route utilizing copper nitrate and sodium sulphide as precursors. The reaction time was kept constant at 12h, varying the reaction temperature from 100°C,

*Corresponding author (E-mail: yuktigupta2397@gmail.com)

125°C, and 150°C. The as-synthesized particles were characterized for structural properties using XRD and SEM. The optical properties were investigated by Ultraviolet-Visible & Photo luminescence spectroscopy. The Commission International de l'Eclairage (CIE) plot revealed that the CIE coordinates of the material lie in the blue region.

2 Materials and Methods

In this study, Copper nitrate trihydrate ($\text{Cu}(\text{NO}_3)_2 \cdot 3\text{H}_2\text{O}$) was purchased from Nice Chemicals and sodium sulphide (Na_2S), was purchased from Loba Chemie, which were used as precursors for Copper and Sulphur respectively. All the chemicals were utilized in their original form without any refinement and deionized (DI) water was used as a solvent during the synthesis. Initially, 0.3M solution of both the precursors were prepared separately, and then Na_2S solution was added dropwise to the $\text{Cu}(\text{NO}_3)_2$ solution. The colour of the $\text{Cu}(\text{NO}_3)_2$ solution changed gradually from blue to teal to black coloured which represents the formation of copper sulphide nanoparticles. The as-prepared nanoparticle solution was transferred to the teflon. The autoclave was kept at different temperatures i.e. 100 °C, 125 °C and 150 °C for 12 h. The obtained CuS precipitates were washed with DI water, transferred to a clean dry watch glass, and dried at 80 °C for 10 h. The samples heated at 100 °C, 125 °C and 150 °C are labelled as CuS_100, CuS_125, CuS_150 respectively.

The XRD (X-ray diffraction) pattern of the as-synthesised CuS nanoparticles is obtained via Rigaku Mini Flex II diffractometer with $\text{Cu K}\alpha$ radiation ($\lambda = 1.54 \text{ \AA}$) to study the phase of the sample was recorded in the range of 10– 90° at a scanning rate of 0.02° min⁻¹. Scanning Electron Microscopy (SEM, Nova Nano SEM 450) is used to study the morphology and the participating elements were confirmed by Energy Dispersive X-Ray (EDX) equipped with electron microscopy. Shimadzu RF-5301PC Spectrofluoro photo meter was used to measure the Photo luminescence (PL) spectra of synthesised nanoparticles. Shimadzu UV-3600 Plus UV-Visible Spectrophotometer is used to study the absorption spectra of nanoparticles at room temperature.

3 Results and Discussion

3.1. Structural analysis

Figure 1 shows the XRD pattern of CuS nanoparticles synthesised at three different temperatures 100 °C, 125 °C and 150 °C. The diffraction peaks of as-synthesised sample are in well agreement with the

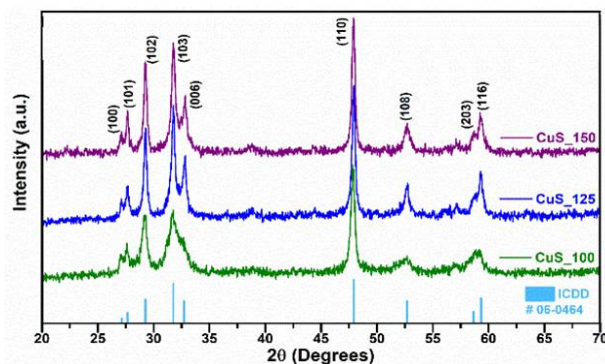


Fig. 1 — XRD pattern of CuS Nanoparticles with temperature as 100°C, 125°C, and 150°C.

Table 1 — XRD Peak parameters calculated for CuS samples

Sample Name	Average FWHM (nm)	Average Crystalline Size (D) (nm)	Average d-spacing (nm)	Lattice Parameter (Å)	
				a = b	c
CuS_100	1.22	9.15	0.23	3.77	16.79
CuS_125	0.60	16.15	0.24	3.78	16.57
CuS_150	0.49	19.5	0.24	3.78	16.38

hexagonal structure of Covellite CuS (ICDD card no. 06-0464). The prominent peaks are obtained at 2θ values 29.25°, 31.77° and 47.90° corresponding to the (102), (103), and (110) planes respectively in all the samples. Also, the intensity of peaks has increased with increasing reaction temperature, but a slight broadening of peaks is observed in the sample at 150 °C. The d-spacing of the prepared samples are calculated using the standard equations and Debye–Scherrer's formula is used for calculation of average crystallite size (D) 30. The value of lattice constants a, b and c matches well with the standard values (i.e., $a=b=3.79 \text{ \AA}$, $c=16.34 \text{ \AA}$) confirming the hexagonal structure. Different parameters calculated from XRD for all three samples are collected in Table 1.

Some additional peaks are found along with the shift of 0.1° with respect to standard data, in the higher diffraction angle in CuS_125 and CuS_150 at the 2θ values 32.72°, 52.70° and 58.65° for the planes (006), (108), and (203) respectively as shown in Fig. 2. The variation of FWHM along with the crystallite size can be clearly seen in Fig. 3. The average d-spacing of the shifted peaks is decreasing by the value of 0.05 Å in CuS_150 as compared to CuS_100.

3.2. Morphological analysis

3.2.1. Scanning Electron Microscopy (SEM) Analysis and Energy Dispersive X-ray (EDX) Analysis

Figure 4 shows the SEM images of the as-synthesised CuS nanoparticles at different reaction

temperatures. The SEM images are obtained at 15kV at a magnification of 13,000 with image size 1µm. Figure 4(a) shows the formation of nanoparticles, the spherical shape becomes more prominent as we move to Fig. 4(b) and Fig. 4(c). The SEM image reveal the presence of agglomeration in the synthesised

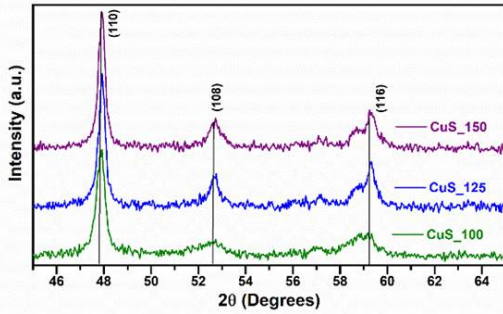


Fig. 2 — Shifting in XRD pattern.

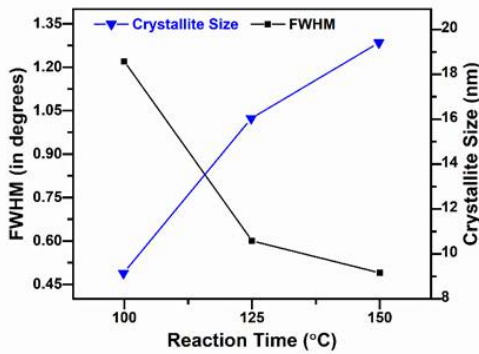


Fig. 3 — Variation of Crystallite size with FWHM.

nanoparticles. The agglomeration increases with increase in reaction temperature. Figure 4 (d)&(f) shows EDX spectra of the samples which confirms the presence of Cu and S as the only elements with no impurity peaks. The atomic % for Cu and S is shown in Fig. 4 (d) & (f) along with the spectra. The ratio of Cu:S is approximately 1:1 in all the three samples but the CuS₁₂₅ matches exactly.

3.3. Optical Properties

3.3.1. Ultraviolet- Visible (UV-Vis.) absorption studies

Figure 5 represents the absorbance spectra of as-synthesised nanoparticles. In the obtained absorbance spectra wavelength range was kept between 290-350 nm. It shows absorbance peak around 300 nm. The energy band gap of nanoparticles is calculated by plot between $(\alpha hv)^{1/2}$ vs $h\nu$ (i.e.Tauc’s plot). This plot can be obtained using Tauc’s equation³¹ as under

$$\alpha hv = C(h\nu - E_g)^n \quad \dots(1)$$

where α signifies coefficient of absorption, $h\nu$ represents energy of photon, E_g denotes optical bandgap, n is $1/2$ for direct allowed transition and C denotes energy-dependent constant.

Fig. 4. SEM image of (a) CuS₁₀₀ (b) CuS₁₂₅ (c) CuS₁₅₀ and EDX spectra of nanoparticles (d) CuS₁₀₀ (e) CuS₁₂₅ (f) CuS₁₅₀. Energy band gap values comes out to be 3.1 eV for CuS₁₀₀, 3.27 eV for CuS₁₂₅, and 2.9 eV for CuS₁₅₀. The band gap value initially increases from CuS₁₀₀ to CuS₁₂₅

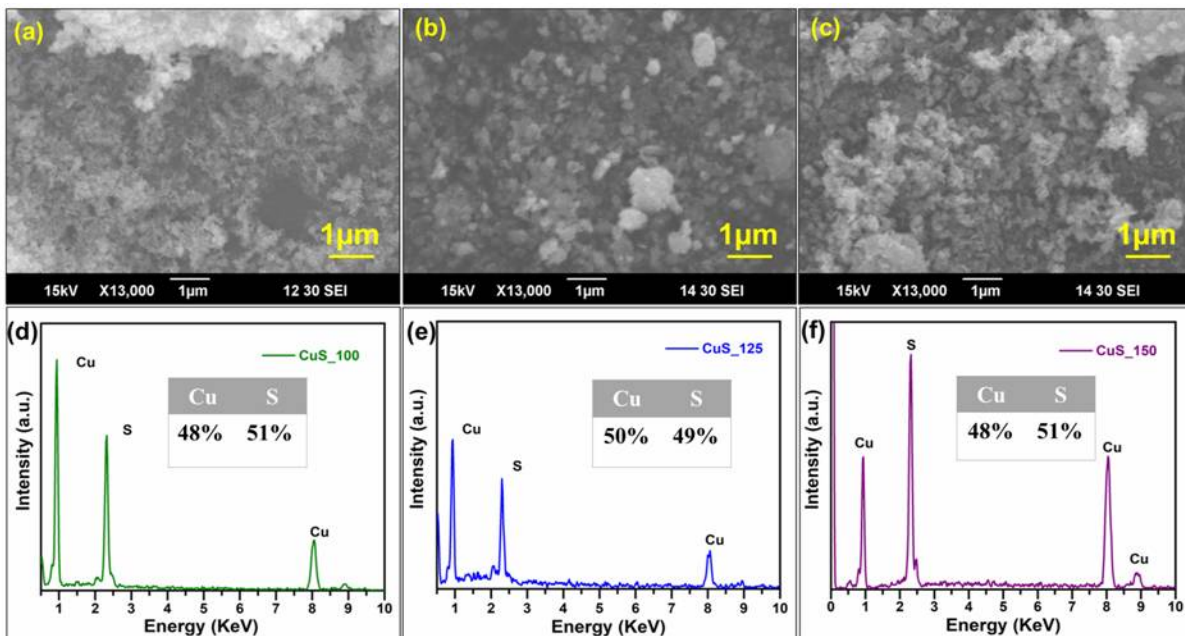


Fig. 4 — SEM image of (a) CuS₁₀₀ (b) CuS₁₂₅ (c) CuS₁₅₀ and EDX spectra of nanoparticles (d) CuS₁₀₀ (e) CuS₁₂₅ (f) CuS₁₅₀.

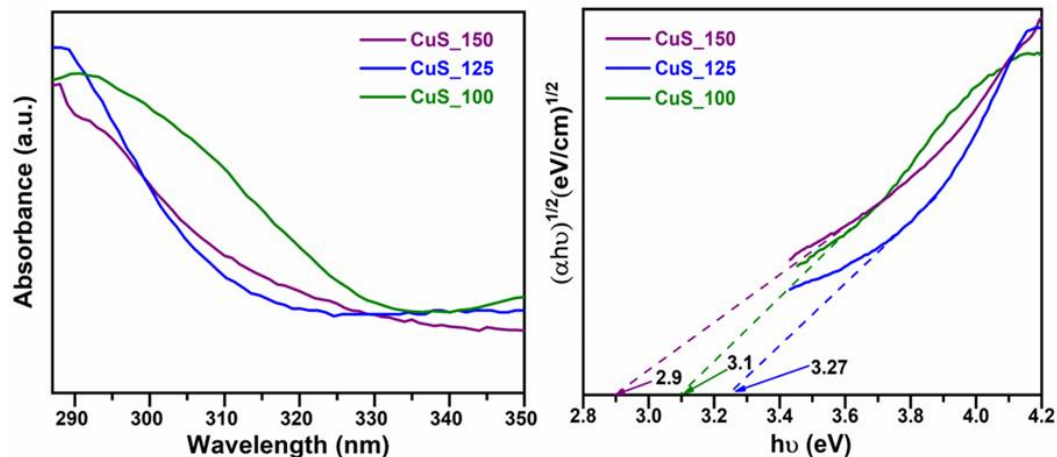


Fig. 5 — Absorption spectra and Tauc's plot of CuS nanoparticles at different temperatures.

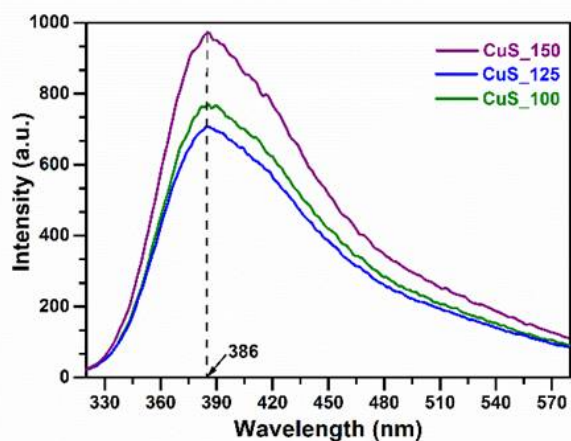


Fig. 6 — PL spectra of samples of CuS nanoparticles.

and then decrease from CuS_125 to CuS_150. The result reveals that CuS_125 has the highest band gap.

3.3.2. Photoluminescence Studies

The Photoluminescence spectra which were collected at room temperature and at an excitation wavelength of 300 nm for all the samples are shown in Fig. 6. The samples give emission peak at 386 nm^{32,33}, but there is variation in intensity with increasing temperature. The PL intensity of CuS_100 and CuS_150 is higher as compared to that of CuS_125. This shows CuS_125 has lower recombination rate which is an appreciable property for optical applications. So, this sample may be a promising candidate to use as optical sensor or LEDs. The Commission International de l'Eclairage (CIE) 1931 chromaticity diagram³⁴ for CuS_100, CuS_125 and CuS_150 is shown in Fig. 7. The chromaticity coordinates are evaluated to be $(x, y) = (0.18, 0.18)$ using PL data which came out to be same for all the three samples.

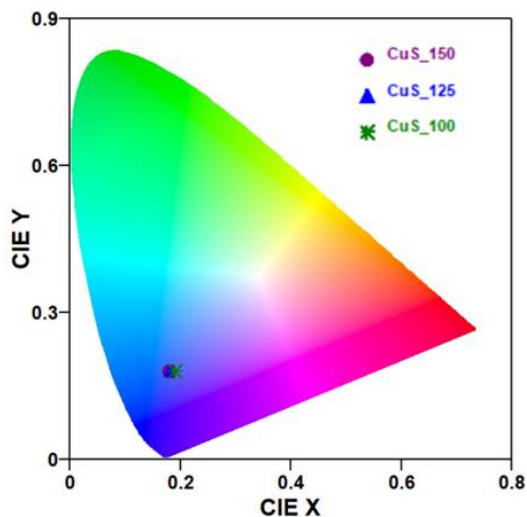


Fig. 7 — CIE chromaticity diagram.

The CIE points lie in blue region of chromaticity diagram, which reveals that the samples emit blue light and hence, can be used in blue LEDs or lamps.

4 Conclusion

In this work, we reported the synthesis of Covellite CuS nanoparticles using copper nitrate trihydrate ($\text{Cu}(\text{NO}_3)_2 \cdot 3\text{H}_2\text{O}$) and Sodium Sulphide (Na_2S) as precursors and DI water as solvent. The samples were placed in a stainless- steel autoclave at various reaction temperatures using hydrothermal process. The effect of reaction temperature was investigated by treating the samples at 100 °C, 125 °C and 150 °C for 12 h. The XRD measurements reveal the peaks of all the three samples match well with the hexagonal phase of CuS. The sample kept at 125 °C shows sharp peaks with higher intensity which shows that the sample was more crystallinity. The crystallite size shows an increasing

trend with increase in temperature. EDX analysis confirms the presence of Cu and S as the only elements in the sample. SEM reveals the nearly spherical shaped morphology along with the presence of agglomeration which is common in nanoparticles. The samples show absorbance around 300 nm which is used as excitation wavelength in Photoluminescence spectra. The study of Tauc's plot reveals that bandgap comes out to be 3.1 eV for CuS_100 TE, 3.27 eV for CuS_125, and 2.9 eV for CuS_150. The result shows CuS_125 has the highest band gap. The emission peak in the PL spectra obtained at an excitation wavelength of 300 nm is located at 386 nm. CuS_125 has lowest intensity which shows the sample has lowest recombination rate and the chromaticity diagram reveals the emission of light in blue region. This indicates that the sample CuS_125 is suitable candidate for BLEDs.

Acknowledgement

Author Yukti is thankful to Director, National Institute of Technology, Kurukshetra for providing Institute fellowship. The author gratefully acknowledges to Dr. Ashish Gupta, Department of Physics, National Institute of Technology, Kurukshetra for constant support. The author also acknowledges Dr. Sanjeev Aggarwal, Director Ion Beam Centre, Kurukshetra University, Kurukshetra for providing UV-Visible spectroscopy facility.

References

- Rani N, & Jaggi N, *Bull Mater Sci*, 43 (2020) 1.
- Khurana K, & Jaggi N, *J Mater Sci Mater Electron*, 31 (2020) 10334.
- Sharma S, Kumar K, Thakur N, Chauhan S, & Chauhan M S, *Bull Mater Sci*, 43 (2020) 1.
- Kaur A, Kaur B, Singh K, Kumar R, & Chand S, *Bull Mater Sci*, 44 (2021) 268.
- Munyai S, Mahlaule G L M, & Hintsho M N C, *Mater Res Express*, 9 (2022) 197.
- Gupta A, Dhakate S R, Gurunathan P, & Ramesha K, *Appl Nanosci*, 7 (2017) 449.
- Lindroos S, & Leskelä M, *Int J Inorg Mater*, 2 (2000) 197.
- Lenggoro IW, Kang YC, Komiyama T, Okuyama K, & Tohge N, & *Japanese J Appl Physics*, 37 (1998) 288.
- Radhakrishnan S, Kim H, & Kim B, *Sensors Actuators B Chem*, 233 (2016) 93.
- Hu XS, Shen Y, Xu LH, Wang LM, & Xing YJ, *J Alloys Compd*, 674 (2016) 289.
- Wang Z, Rafai S, Qiao C, Jia J, Zhu Y, Ma X, & Cao C, *ACS Appl Mater Interfaces*, 11 (2019) 7046.
- Zeinodin R, & Jamali-Sheini F, *Phys B Condens Matter* 570 (2019) 148.
- Balakrishnan A, Groeneveld J D, Pokhrel S, & Mädler L, *Chem - A Eur J*, 27 (2021) 6390.
- Mu C F, Yao Q Z, Qu X F, Zhou G T, Li M L, & Fu S Q, *Colloids Surfaces A Physicochem Eng Asp*, 371 (2010) 14.
- Riyaz S, Parveen A, & Azam A, *Perspect Sci*, 8 (2016) 632.
- Yadav S, & Bajpai P K, *Soft Nanosci Lett*, 8 (2018) 9.
- Gao L, Wang E, Lian S, Kang Z, Lan Y, & Wu D, *Solid State Commun*, 130 (2004) 309.
- Sabeeh H, Aadil M, Zulfiqar S, Aadil M, Zulfiqar S, Rasheed A, Al K N F, Philips A O, Haider S, Warsi M F, & Shakir I, *Ceram Int*, 47 (2021) 13613.
- Xu H, Wang W, & Zhu W, *Mater Lett*, 60 (2006) 2203.
- Yadav S, Shrivastava K, & Bajpai P K *J Alloys Compd*, 772 (2019) 579.
- Zhong R, Peng C, Chen L, Yu N, Liu Z, ZHU M, He C, & Chen Z, *RSC Adv*, 6 (2016) 40480.
- Deb S, & Kalita P K, *J Mater Sci Mater Electron*, 32 (2021) 24125.
- Saranya M, Ramachandran R, Samuel E J J, Jeong S K, & Grace A N, *Powder Technol*, 279 (2015) 209.
- Bakr M, & Abdel K MH, *Mater Chem Phys*, 241(2020) 122285.
- Ajibade PA, *J Nanotechnol*, 2019 (2019) 11.
- Seoudi RA, Shabaka A, Eisa WH, Anies B, & Farage NM, *Phys B Phys Condens Matter*, 405(2010) 919.
- Goswami M, Adhikary NC, & Bhattacharjee S, *Opt - Int J Light Electron Opt*, 158 (2018) 1006.
- Priya M, Geetha S, Ramamurthi A, *J Mater Sci Mater Electron*, 29(2018) 658.
- Abbas S, Basma H, Bhoukhari JA, & Awad R, *Appl. Phys. A*, 127 (2021) 505.
- Sadiq I, Khan I, Rebrov E V, Ashiq MN, Naseem S, & Rana MU, *J Alloys Compd*, 570(2013) 7.
- Tauc J, & Mentha A, *J Non Cryst Solids*, 8(1972) 569.
- Chaki SH, Tailor JP, & Deshpande M *Adv Sci Lett*, 20 (2014) 959.
- Gupta A, Khosla N, Amit VG, & Annapurna SK, *Appl Nanosci*, 10 (2020) 4191.
- Gangwar AK, Gupta A, Kedawat G, Kumar P, Singh BP, Singh N, Srivastava AK, Dhakate SR & Gupta BK, *Eur J Chem*, 24(2018) 9477.